Aerosol Sci Eng
DOI 10.1007/s41810-017-0007-z

ORIGINAL PAPER

Methanol Extracted Brown Carbon in $PM_{2.5}$ Over Xi'an, China: Seasonal Variation of Optical Properties and Sources Identification

Zhenxing Shen[1,2] · Yali Lei[1] · Leiming Zhang[3] · Qian Zhang[1] · Yaling Zeng[1] · Jun Tao[4] · Chongshu Zhu[2] · Junji Cao[2] · Hongmei Xu[1] · Suixin Liu[1]

Received: 22 December 2016 / Revised: 1 April 2017 / Accepted: 3 May 2017

Abstract Aerosol optical properties, including absorption coefficient (b_{abs}), absorption Ångström exponent (AAE), and mass absorption coefficient (MAC), of methanol extracts in $PM_{2.5}$ samples were measured at an urban site in Xi'an, northwest China in a winter and summer season. Water soluble ions, organic carbon (OC), element carbon, eight carbon fractions, levoglucosan, and 13 polycyclic aromatic hydrocarbons were also determined to explore the sources of brown carbon (BrC) in $PM_{2.5}$. b_{abs} at 365 nm wavelength showed a clear seasonal variation with much higher value in winter than summer. High levoglucosan and K^+ concentrations in winter and their good correlations with b_{abs} inferred the important contribution of biomass burning to BrC. Good correlations between b_{abs} and OC1, OC2, OC3, or OP indicated the mixed sources of biomass burning and coal combustion for BrC. Relatively poor correlations were found between b_{abs} and indeno[1,2,3-cd]pyrene (IP) or Benzo[ghi]-perylene (BghiP), indicating limited contribution of vehicle exhaust to BrC. Seasonal distribution of AAE indicated that secondary organic carbon (SOC) BrC was mainly fresh SOC in winter but a mix of fresh and aged SOC in summer. MAC of BrC in winter was more than double of that in summer, suggesting that BrC from biomass burning and fresh SOC were stronger light absorbing in winter than the aged SOC in summer. A 7-wavelength Aethalometer model AE31 was used to evaluate the seasonal variations of b_{abs} for BrC (370 nm) and black carbon (BC) (880 nm). BrC and BC were both important in light absorption in winter, but BC prevailed over BrC in summer.

Keywords Brown carbon · Optical properties · Biomass burning · Secondary organic carbon

1 Introduction

Black carbon (BC) strongly absorbs solar radiation, whereas organic carbon (OC) was considered as purely scattering solar radiation (Bond et al. 2011). However, recent studies revealed that a portion of OC, referred to as brown carbon (BrC), also absorbs solar radiation substantially at ultraviolet wavelengths (Bahadur et al. 2012; Lack et al. 2012). BrC is organic matter including nitro-phenol derivatives, humic-like substances (HULIS), water and organic solvent extracts of ambient particulate matter (PM), amorphous carbon spheres from combustion process, and secondary organic carbon (SOC) (Desyaterik et al. 2013; Hoffer et al. 2006; Chakrabarty et al. 2010; Laskin et al. 2014, 2015; Teich et al. 2016).

Due to the complex chemical components and origins of BrC, it is difficult to determine its mass fraction in PM. However, it is feasible to obtain BrC optical properties, including absorption coefficient (b_{abs}), absorption Ångström exponent (AAE), and mass absorption coefficient of (MAC), which are needed to understand the characteristics

✉ Zhenxing Shen
zxshen@mail.xjtu.edu.cn

1 Department of Environmental Science and Engineering, Xi'an Jiaotong University, Xi'an 710049, China

2 Key Lab of Aerosol Chemistry and Physics, Institute of Earth Environment, Chinese Academy of Sciences, Xi'an 710049, China

3 Air Quality Research Division, Science and Technology Branch, Environment and Climate Change Canada, Toronto, Canada

4 South China Institute of Environmental Sciences, Ministry of Environmental Protection, Guangzhou, China

Published online: 10 May 2017

of BrC and its impact on climate. A popular optical measurement method was to isolate BrC through water or organic solvent extraction, followed by BrC absorption measurement in the extracts (Hecobian et al. 2010; Cheng et al. 2016). An alternative optical estimation of BrC is using an optical instrument (such as BC online measurement) without isolating from BC, which involves attributing total aerosol absorption to BC and BrC absorption (Sandradewi et al. 2008; Favez et al. 2010). This method disregards the impact of BC mixing state on its light absorption, and uncertainties of this method are described in Lack and Langridge (2013).

Biomass burning from cooking and winter heating was a major contributor to regional air pollution in northwest China (Shen et al. 2009; Sun et al. 2017), but a few studies have addressed $PM_{2.5}$ BrC in this region. In the present study, optical measurements on methanol extracts of $PM_{2.5}$ samples were conducted to gain some insight of seasonal variations of optical properties and BrC origins over Xi'an, China. In addition, measurements of 7-wavelength BC were also conducted to compare the light absorption between BrC and BC.

2 Materials and Methods

2.1 $PM_{2.5}$ Samples Collection

The sampling site was located in the southeastern part of downtown Xi'an surrounded by residential areas and major traffic roads. The area frequently experiences heavy air pollution produced locally as well as from regional transport. $PM_{2.5}$ samples were collected on quartz filters by a high-volume ($\sim$1.13 m^3 min^{-1}) air sampler (HVS-$PM_{2.5}$, Thermo-Anderson Inc.) at the rooftop of a 15-m high building. One 24-h $PM_{2.5}$ sample (starting at 9:30 AM) was collected every week in a summer (from 2 June to 31 October 2015) and a winter (from 30 November 2015 to 28 February 2016) season. Detailed description of the sampling site and sampling method can be found in Shen et al. (2017).

2.2 Chemical Species Measurements

Nine ionic species (SO_4^{2-}, NO_3^-, Cl^-, F^-, Na^+, NH_4^+, K^+, Mg^{2+}, and Ca^{2+}) in $PM_{2.5}$ samples were determined by ion chromatography (Dionex 600, Dionex Corp, Sunnyvale, USA). The detailed analysis processes and quality assurance and quality control for ions can be found in Shen et al. (2009). Organic carbon (OC) and elemental carbon (EC) in $PM_{2.5}$ samples were analyzed using Thermal and Optical Carbon Analyzer (Model 2001, Atmoslytic, Inc., US) with IMPROVE (Interagency Monitoring of Protected Visual Environment) thermal/optical reflectance (TOR) protocol. Four OC fractions (OC1, OC2, OC3, and OC4 at 140, 280, 480, and 580 °C, respectively, in a non-oxidizing helium atmosphere) and three EC fractions (EC1, EC2, and EC3 at 580, 740, and 840 °C, respectively, in a 2% oxygen/98% helium atmosphere) were determined in this study. During volatilization of OC, part of OC was converted pyrolytically to EC (this fraction of OC was named as OP) (Chow et al. 2004). OC was defined as OC1 + OC2 + OC3 + OC4 + OP and EC as EC1 + EC2 + EC3-OP. The detailed analysis processes can be found in Cao et al. (2003).

Levoglucosan was measured using the method of improved high-performance anion-exchange chromatography (HPAEC) with pulsed amperometric detection (PAD). The HPAEC-PAD system was composed of a Dionex ICS-3000 series ion chromatograph (Dionex Corp., Sunnyvale, CA, USA), SP (quaternary pump and degasser), DC (column compartment), and ED (electrochemical detector and gold electrode) units. The detection limit was 0.002 mg L^{-1} for levoglucosan. More details about this analyzer including its calibration were given by Shen et al. (2017).

Thirteen priority polycyclic aromatic hydrocarbon (PAHs) species as listed by the United States Environment Protection Agency were determined, including fluorine (Flu), phenanthrene (Phe), anthracene (Ant), fluoranthene (FLA), pyrene (Pyr), benzo[a]fluoranthene (BaF), chrysene (Chr), benzo[b]fluoranthene (BbF), benzo[k]fluoranthene (BkF), benzo[a]pyrene (BaP), indeno[1,2,3-cd]pyrene (IP), dibenzo[a,h]anthracene (dBahA), and Benzo[g,hi]-perylene (BghiP). A quarter of one 47 mm diameter filter was extracted with dichloromethane (DCM) using ultrasonic agitation and filtered to determine PAHs levels. This procedure was repeated three times. Surrogate PAHs (consisted of naphthalene-D8; acenaphthene-D10; phenanthrene-D10; chrysene-D12, and perylene-D12 standards) were added prior to extraction. The organic extracts were combined, and the solvent was removed using a rotary evaporator. Interfering compounds, including aliphatic hydrocarbons, organic acid, etc., were removed by homemade silicon column (alumina:silica gel:anhydrous sodium sulfate was equal to 3:2:1). The extracts were then concentrated using rotoevaporation followed by evaporation under purified nitrogen; internal standard hexamethylbenzene was added and the volume was adjusted to 1 mL (Mesquita et al. 2014; Gao et al. 2015). PAHs were analyzed using gas chromatography with mass selective detection (GC/MS). The chromatographic conditions were as follows: injector temperature 290 °C and detector temperature 250 °C. The temperature ramp was an initial oven temperature of 50 °C maintained for 2 min, increased at 5 °C/min to 280 °C, and then increased at 3 °C to a maximum of 300 °C for 10 min.

The aerosol sampler was checked and calibrated regularly during the sampling period, and field blank filters

were collected to correct for background concentrations. Procedure and reagent blanks were measured and subtracted from the results. In addition, surrogate standards were added to all the samples (including QA samples) to monitor procedural performance and matrix effects. Average recoveries for surrogate PAHs naphthalene-d10, acenaphthylene-d10, anthracene-d10, phenanthrene-d10, chrysene-d12, and benzo[a]pyrene-d12 were 27, 51, 132, 95, and 38%, respectively. The recoveries were acceptable and comparable to those reported for trace organic analysis (Shen et al. 2011). One in every ten samples was randomly chosen for repeating analysis and the deviation was controlled to be less than 5% for repeat analysis (Rajput et al. 2011). The GC–MS was tuned before and after the measurements to ensure the sensitivity and stability (Meng and Anderson 2010).

2.3 Optical Properties of $PM_{2.5}$ BrC by Water and Methanol Extracts

The light absorption spectra of the water and methanol extracts were measured with a UV–Vis spectrophotometer (UV-6100 s) with 10-cm optical paths in the individual solvent. Each solvent was separately extracted from five punches of aerosol samples in high purity water (a resistivity of 18.3 MΩ) and methanol (HPLC Grade, Fisher Chemical). Each solvent was sonicated for 1 h and shaken by mechanical shaker for 1 h, and all the extracts were filtered 1–3 times through a 25-mm diameter 0.45-μm pore syringe filter (Puradisc 25 TF, PTFE membrane) to remove insoluble components and filter remnants generated during the extraction process.

Absorption spectra of aqueous extracts of aerosols (representing bulk methanol-soluble organic carbon) have been used to assess the absorption coefficient (b_{abs}) as described by Liu et al. (2013) and Srinivas and Sarin (2014). b_{abs} is calculated according to:

$$b_{abs(\lambda)} = (A_\lambda - A_{700}) \times (V_{ext} \times \text{Portions}) \times \ln(10)/(V_{aero} \times L),$$

where b_{abs} is expressed in the unit of Mm^{-1} (or 10^{-6} m^{-1}). A_λ and A_{700} correspond to measured absorbance at specified λ and 700 nm, respectively. V_{ext} refers to volume of the aqueous extract (50 mL). V_{aero} corresponds to sampling volume, and L is the path length of the cell (10 cm). Absorbance at 365 nm was used to estimate the absorption coefficient (b_{abs}) of light absorbing soluble (water and methanol) organic carbon (also referred to as BrC) (Liu et al. 2013).

The relationship between wavelength-dependent absorption Ångström exponent (AAE) and $b_{abs\ (365\ nm)}$ of BrC in the aqueous extracts is described the following Hecobian et al. (2010) and Teich et al. (2016):

$$b_{abs} = K \times \lambda^{-AAE}.$$

Here, K refers to a constant value and λ denotes wavelength of BrC. In this study absorption Ångström exponent (AAE) is calculated by a linear regression fit between log b_{abs} and log λ in the wavelength range of 330–400 nm.

The steep increase of ambient and combustion aerosol AAE values can also be used as an indicator for identifying specific BrC sources (Saleh et al. 2014; Sandradewi et al. 2008). An AAE value in the range of 1–2.9 was derived from coal burning aerosols and 6–8 from biomass burning aerosols (Bond 2001; Hecobian et al. 2010). Higher AAE values (6.9–11.4) of BrC were from the incomplete biofuel burning in methanol extracts (Chen and Bond 2010). The prominent differences in AAE values between the aged and fresh aerosols suggested that the formation mechanisms also played important roles in BrC absorption parameters (Zhang et al. 2011; Bones et al. 2010).

For the methanol extracts, only light absorption spectra were analyzed, since the use of an organic solvent prohibits determining carbon mass in these solutions. As a consequence, mass absorption coefficient (MAC) of BrC (m^2 g^{-1}) at 365 nm was calculated based on:

$$MAC_\lambda = b_{abs}(365nm)/OC.$$

2.4 b_{abs} at 370 nm and 880 nm

Comparison of light absorption between BrC and BC will help to understand their roles in environmental and climate change. Light absorption coefficient (b_{abs}) is the most important parameter for BC determination, which can be obtained at seven wavelengths (i.e., 370, 470, 520, 590, 660, 880, and 950 nm) using an Aethalometer model AE31. According to Beer–Lambert's law, b_{abs} is defined as:

$$I = I_0 e^{-b_{abs} \cdot x},$$

where I_0 and I are the light intensities after passing through a blank quartz fiber filter and the collected particles on the filters with the thickness x, respectively. Similar to other filter-based absorption instruments, the b_{abs} of AE31 needs to be corrected for two kinds of errors, including scattering effect by the fiber filter substrates (Collaud Coen et al. 2010) and filter mass loading by the accumulation of light absorbing particles. In this study, mass loading effect was corrected following the correction process presented by Virkkula et al. (2007). The multiple scattering of the light beam at the filter fibers strongly depends on the filter material and can be corrected by an empirical coefficient (2.14) (Drinovec et al. 2014; Cheng and Yang 2015).

Olson et al. (2015) segregated BC and optical-BrC by projecting the absorption at higher (880 nm) to lower wavelengths of the spectrum measured by AE31. The absorption at 880 nm is attributed to BC absorption only, while absorption at lower wavelength (370 nm) is attributed to both BC and BrC absorption. The simple extrapolation method using AAE has been used in several studies and was described in detail by Lack and Langridge (2013). We projected the absorption coefficient at 880–370 nm wavelengths using a value of 1 for AAE to estimate the BC contribution of the bulk absorption coefficient. Using AAE = 1 projection, the absorption coefficient of BC component ($b_{\text{abs-BC}}$, AAE = 1, 370 nm) of the bulk absorption coefficient can be calculated for 370 nm wavelength; subtracting this value from the bulk absorption coefficient $b_{\text{abs, 370 nm}}$ results in the net optical-BrC absorption coefficient. The calculation of AAE and $b_{\text{abs-BrC, 370 nm}}$ is as follows:

$$\text{AAE} = -(\ln(b_{\text{abs}}(\lambda_1)) - \ln(b_{\text{abs}}(\lambda_2))/(\ln(\lambda_1) - \ln(\lambda_2)))$$

$$b_{\text{abs-BrC,370 nm}} = b_{\text{abs,370 nm}} - b_{\text{abs-BC,AAE=1,370 nm}}.$$

3 Results and Discussion

3.1 Comparison of Light Absorption Between Water Extracts and Methanol Extracts

Light absorption of water and methanol extracts was investigated, as shown in Fig. 1. Both methods exhibited much higher b_{abs} at short wavelength than long wavelength, indicating light absorption by BrC in this spectrum. Methanol extracts showed higher b_{abs} than water extracts, demonstrating the more suitability of using methanol extracts to measure the optical properties of $PM_{2.5}$ BrC. Cheng et al. (2016) reported that methanol extracted organic compounds constituted nearly 85% of OC, while water extracts constituted about 40% of OC. In the present study, the ratio of b_{abs} at 365 nm between water and methanol extracts from five selected samples ranged from 0.29 to 0.53 with an average of 0.37 (Table 1). Such results inferred that the light absorption by BrC was underestimated by more than 50% if using water extracts compared with methanol extracts. Therefore, the optical properties of $PM_{2.5}$ BrC by methanol extracts were discussed in the following sections.

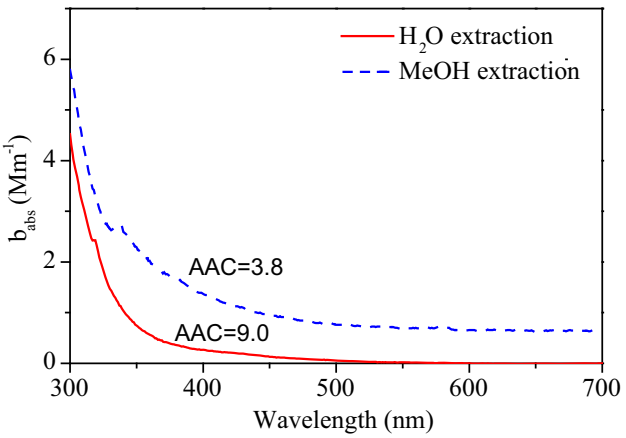

Fig. 1 Comparison of AAE between water (*red line*) and methanol (*blue line*) extracts (color figure online)

3.2 Seasonal Variations of Optical Properties of BrC

Table 2 shows the summer and winter levels of b_{abs}, AAE, MAC, and $PM_{2.5}$ chemical components. Mean $b_{\text{abs, 365 nm}}$ in winter was about six times of that in summer, indicating more abundance of BrC in $PM_{2.5}$ samples in winter. Biomass burning for heating in rural areas in winter should have contributed to the high BrC (Sun et al. 2017). High levels of OC and biomass burning marker (K^+ and levoglucosan) in winter also supported this hypothesis (Table 2). The AAE values were at similar levels between winter and summer, although more scattered values (4.02–16.3) were found in summer than winter (6.1–11.0). AAE value can be a good indicator for BrC sources. For example, the AAE of water extracted BrC for coal combustion and biomass burning source $PM_{2.5}$ samples were 4.4 and 7.4, respectively, in Xi'an, China (Shen et al. 2017). Chen and Bond (2010) reported that the AAE of BrC for biomass burning methanol extracts ranged from 7 to 16. The AAE for BrC in Beijing averaged 7.1 in winter, which also demonstrated by biomass burning contribution (Cheng et al. 2016). In addition, secondary organic carbon (SOC) was also an important contributor to BrC, and the AAE of aged SOC-BrC (4.7) was much lower than that of fresh SOC-BrC (8.6–17.8) (Bones et al. 2010). High AAE found in the present study implied important contributions of biomass burning to BrC. In addition, high SOC levels occurred in both summer and winter $PM_{2.5}$, despite different SOC formation mechanisms in different seasons (Zhang et al. 2015; Shen et al. 2017). The most important classes of light absorbing SOC compounds, such as nitro-phenols, aromatic carbonyls, and chromophores, were produced from photochemical processes with higher oxidant levels or aqueous heterogeneous conversion (Hecobian et al. 2010; Desyaterik et al. 2013). More scattered summer AAE values indicated the contribution of both aged and fresh SOC to BrC. In contrast, winter AAE was mostly from fresh SOC.

Table 1 Comparison of absorption coefficient (b_{abs}) at 365 nm between water and methanol extracts in $PM_{2.5}$ over Xi'an

	WSOC		MSOC		$b_{abs\text{-}WSOC}/b_{abs\text{-}MSOC}$
	$b_{abs,\ 365\ nm}$	AAE (330–400 nm)	$b_{abs,\ 365\ nm}$	AAE (330–400 nm)	
Sample 1	1.04	9.05	2.59	3.84	0.40
Sample 2	1.06	10.15	1.99	5.40	0.53
Sample 3	6.23	6.40	20.68	6.40	0.30
Sample 4	5.38	6.62	17.29	6.54	0.31
Sample 5	1.54	7.50	5.30	9.16	0.29

Table 2 Seasonal average $b_{abs,\ 365\ nm}$, AAE, $MAC_{365\ nm}$ of BrC, and mass concentrations of chemical species for $PM_{2.5}$ samples

	Summer		Winter	
	Average	Standard deviation	Average	Standard deviation
$b_{abs,\ 365\ nm}$ (Mm^{-1})	3.50	2.13	21.08	7.28
AAE	7.76	3.19	7.24	1.22
$MAC_{365\ nm}$ ($m^2\ g^{-1}$)	0.59	0.42	1.46	0.30
K^+ ($\mu g\ m^{-3}$)	0.27	0.13	0.55	0.20
OC ($\mu g\ m^{-3}$)	6.23	2.24	14.41	4.33
Levoglucosan ($ng\ m^{-3}$)	100.38	35.87	268.52	99.29
SO_4^{2-} ($\mu g\ m^{-3}$)	6.71	4.46	6.71	7.23
BaP ($ng\ m^{-3}$)	2.97	2.85	10.21	11.68
IP ($ng\ m^{-3}$)	3.32	11.24	3.00	4.52
BghiP ($ng\ m^{-3}$)	2.76	5.02	2.58	1.72

MAC of BrC in winter was more than double of that in summer, implying that BrC from biomass burning and fresh SOC were stronger light absorbing in comparison with aged SOC. Cheng et al. (2016) reported the similar level of MAC for methanol extracts in winter in Beijing. It should be noted that in Cheng et al. (2016), the methanol extract b_{abs} was normalized by methanol-soluble organic carbon (MSOC) rather than OC. Therefore, our study should have underestimated the MAC when using OC. If assuming an MSOC versus OC ratio of 0.85 (Cheng et al. 2016), MAC in the present study was then corrected to be 0.69 $m^2\ g^{-1}$ for summer and 1.72 $m^2\ g^{-1}$ for winter. In another study in Georgia, U.S. where SOC was mainly influenced by biogenic emissions, relatively low MAC ranging from 0.3 to 0.5 $m^2\ g^{-1}$ was found in summer (Liu et al. 2013; Zhang et al. 2011). Thus, BrC measured in the present study was identified to be mainly associated with anthropogenic emissions based on its higher light absorbing ability in comparison with BrC from biogenic sources. Besides, fresh SOC also prevailed over aged SOC.

3.3 The Relationship Between b_{abs} of BrC with $PM_{2.5}$ Chemical Components

As levoglucosan and water soluble K^+ were good markers for biomass burning (Shen et al. 2009; Zhang et al. 2014; Tao et al. 2016), good correlations between b_{abs} of BrC and these tracers can provide some insights on biomass burring sources (Fig. 2). Strong correlations were, indeed, found, indicating the important contribution of biomass burning to $PM_{2.5}$ BrC. In fact, maize and wheat straw burning for cooking and heating in rural areas of Xi'an influenced heavily on urban and regional air quality, and high concentrations of K^+, levoglucosan, and water soluble organic carbon (WSOC) were observed in PM samples in the previous studies (Shen et al. 2009, 2014; Zhang et al. 2014; Sun et al. 2017). Maize straw smoldering for rural heating in Guanzhong Plain was known to be an important source of $PM_{2.5}$ BrC over Xi'an (Shen et al. 2017). High winter BrC levels will influence environment and climate on urban and downwind areas for its strong light absorbing. As the traditional smoldering for heating in rural areas around Xi'an was one of the major sources for winter BrC, clean and high efficient combustion technologies should be developed in near future to reduce BrC emissions.

Carbon abundances in each of the eight carbon fractions differ by carbon sources (Cao et al. 2005). Prior literature reported that OC1, OC2, and OP were abundant in biomass burning source samples; OC2, OC3, and EC1 were enriched in coal combustion emissions; and OC4, EC1, EC2, and EC3 were strongly related with vehicle exhausts (Cao et al. 2005). In the present study, the relationship between b_{abs} of BrC and eight carbon fractions (OC1–OC4, OP, EC1, EC2, and EC3) were investigated to gain some insight of the sources of BrC. Strong positive correlations were found between b_{abs} and OC1 ($r = 0.94$, $P < 0.0001$),

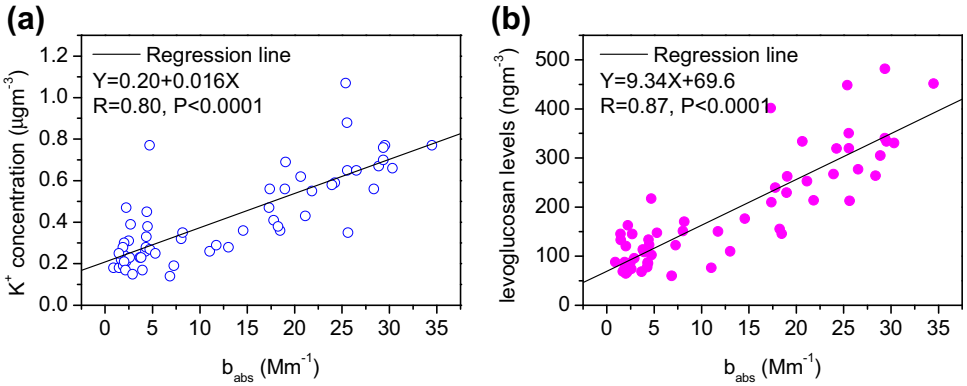

Fig. 2 Relationship between b_{abs} and water soluble K^+ or levoglucosan

OC2 ($r = 0.93$, $P < 0.0001$), OC3 ($r = 0.73$, $P < 0.0001$), OP ($r = 0.93$, $P < 0.0001$), and EC1 ($r = 0.94$, $P < 0.0001$). In contrast, correlation between $b_{abs,\ 365}$ and OC4 was relatively poor, and between $b_{abs,\ 365}$ and EC2 or EC3 was the worst. Therefore, the correlation between b_{abs} and the eight carbon fractions inferred the important contributions of biomass burning and coal combustion to $PM_{2.5}$ BrC. In contrast, the contribution from primary emissions of vehicle exhausts was minor. This was especially the case from diesel vehicle emissions, as seen from the lowest concentrations of EC2 and EC3, which are typical tracers of diesel vehicle emissions (Cao et al. 2005).

Jacobson (1999) attributed the UV absorption to organic species, such as nitrated aromatics, benzaldehydes, benzoic acids, and PAHs. Nitrated aromatic compounds, PAHs, and benzaldehydes were found to be the most effective UV absorbers in terms of their imaginary refractive indices and absorption wavelengths. In this study, 13 PAHs were determined to reveal the possible sources of BrC. The measured total PAHs concentration was 85.5 ng m^{-3} in summer and 118.6 ng m^{-3} in winter. Certain individual PAHs can be taken as tracers for specific emission sources. For example, high level of BaP was mainly from coal combustions (Sawicki 1962); abundance of IP was the typical component from diesel vehicle emissions, and enrichment of BghiP was an indicator of gasoline vehicle emissions (Guo et al. 2005). Strong positive relationship between b_{abs} and BaP ($r = 0.71$, $P < 0.0001$) indicated the important contribution of coal burning to BrC. In contrast, the correlation coefficient between b_{abs} and IP ($r = 0.46$, $P = 0.0002$) or BghiP ($r = 0.33$, $P = 0.009$) was lower than that with BaP, supporting the above conclusion that vehicle emission was not an important source of BrC.

3.4 Comparison of Light Absorption at 370 nm Versus 880 nm

It is challenging to use a 7-wavelength Aethalometer model AE31 or AE33 to accurately investigate the optical absorption of BrC and BC, because BC, BrC, and mineral dust all have relatively strong light absorption overlapped at UV wavelength (Andreae and Gelencser 2006). However, a comparison of light absorption at 370 nm (BrC) versus 880 nm can be used to evaluate the seasonal variation between BrC and BC to some extent. Figure 3 shows the seasonal variation of $b_{abs\text{-}BrC,\ 370\ nm}$ and $b_{abs\text{-}BC,\ 880\ nm}$. $b_{abs\text{-}BrC,\ 370\ nm}$ in winter was over six times of that in summer, indicating abundance of BrC in PM in winter. This was consistent with the above conclusion that coal combustion and biomass burning contributed abundance of BrC. In contrast, seasonal difference in $b_{abs\text{-}BC,\ 880\ nm}$ was not as significant as in $b_{abs\text{-}BrC,\ 370\ nm}$, since $b_{abs\text{-}BC,\ 880\ nm}$ in winter was only 1.6 times of that in summer. The smaller seasonal difference in BC should be mainly caused by the enriched OC in comparison with EC or BC in winter heating. For example, Cachier et al. (1989) reported much higher OC/EC ratio for biomass burning (9.0) in comparison with coal combustion (2.7) and vehicle emission (1.1) (Watson et al. 2001). In the present study, winter OC/EC ratio was 4.1 on average, indicating heavily influenced BrC from winter heating (e.g., coal burning and smoldering biomass burning) but not BC. It is worth noting that mean $b_{abs\text{-}BrC,\ 370\ nm}$ and $b_{abs\text{-}BC,\ 880\ nm}$ were in the same level at about 43 Mm^{-1} in winter, indicating that light absorption by BrC and BC was both important. However, in summer $b_{abs\text{-}BC,\ 880\ nm}$ prevailed over $b_{abs\text{-}BrC,\ 370\ nm}$ due to no biomass burning for heating, and BC from traffic emissions dominated PM light absorption. As a result, controlling biomass smoldering for heating and vehicle exhaust can reduce light absorbing materials effectively.

4 Conclusions

Seasonal contrasts in optical properties of BrC extracted by Methanol were investigated over Xi'an, northwest China. Methanol extract method was more effective in comparison with water extract method, and light absorption of BrC was

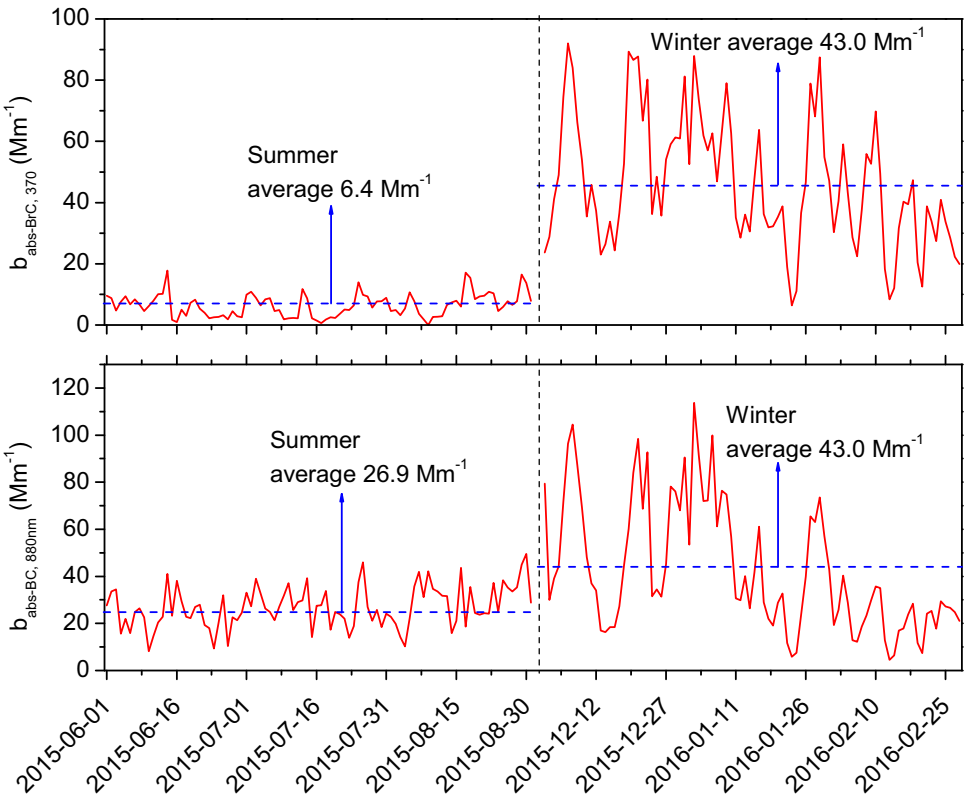

Fig. 3 Comparison of light absorption between BrC (370 nm) and BC (880 nm) measured by 7-wavelength Aethalometer

underestimated by more than one-third if using water extract method. High b_{abs} of BrC was observed in winter, caused by emissions from biomass burning for heating, as supported by the strong correlation between b_{abs} and related emission chemical markers (levoglucosan, K^+, OC1, OC2, OC3, OP, and BaP). SOC-BrC was a mix of aged and fresh SOC in summer, but mostly fresh SOC in winter. As the BrC origins are complicated, the strong UV absorption components (such as nitrated aromatic compounds and benzaldehydes) should be investigated to trace the origins of BrC in the future. In addition, size-dependent optical properties of BrC also need to be obtained to understand its potential environmental impacts.

Acknowledgements This research was supported by the National Natural Science Foundation of China (41573101), Natural Science Foundation of Shaanxi Province, China (2016ZDJC-22), the Fundamental Research Funding for Central Universities in China (xkjc2015002), and the Key Lab of Aerosol Chemistry and Physics of the Chinese Academy of Sciences.

References

Andreae MO, Gelencser A (2006) Black carbon or brown carbon? The nature of light-absorbing carbonaceous aerosols. Atmos Chem Phys 6:3131–3148

Bahadur R, Praveen PS, Xu Y, Ramanathan V (2012) Solar absorption by elemental and brown carbon determined from spectral observations. Proc Natl Acad Sci U S A 109:17366–17371

Bond TC (2001) Spectral dependence of visible light absorption by carbonaceous particles emitted from coal combustion. Geophys Res Lett 28(21):4075–4078

Bond TC, Zarzycki C, Flanner MG, Koch DM (2011) Quantifying immediate radiative forcing by black carbon and organic matter with the specific forcing pulse. Atmos Chem Phys 11:1505–1525

Bones DL, Henricksen DK, Mang SA, Gonsior M, Bateman AP, Nguyen TB, Cooper WJ, Nizkorodov SA (2010) Appearance of strong absorbers and fluorophores in limonene-O_3 secondary organic aerosol due to NH_4^+-mediated chemical aging over long time scales. J Geophys Res 115(D5):D05203

Cachier H, Bremond MP, Buat-Menard P (1989) Carbonaceous aerosols from different tropical biomass burning sources. Nature 340:371–373

Cao JJ, Lee SC, Ho KF, Zhang XY, Zou SC, Fung K, Chow JC, Watson JG (2003) Characteristics of carbonaceous aerosol in Pearl River Delta Region, China during 2001 winter period. Atmos Environ 37:1451–1460

Cao JJ, Wu F, Chow JC, Lee SC, Li Y, Chen SW, An ZS, Fung KK, Watson JG, Zhu CS, Liu SX (2005) Characterization and source apportionment of atmospheric organic and elemental carbon during fall and winter of 2003 in Xi'an, China. Atmos Chem Phys 5:3127–3137

Chakrabarty RK, Moosmüller H, Chen LWA, Lewis K, Arnott WP, Mazzoleni C, Dubey MK, Wold CE, Hao WM, Kreidenweis SM (2010) Brown carbon in tar balls from smoldering biomass combustion. Atmos Chem Phys 10:6363–6370

Chen Y, Bond TC (2010) Light absorption by organic carbon from wood combustion. Atmos Chem Phys 10(4):1773–1787

Cheng YH, Yang LS (2015) Correcting aethalometer black carbon data for measurement artifacts by using inter-comparison

methodology based on two different light attenuation increasing rates. Atmos Meas Tech Discuss 8:2851–2879
Cheng Y, He KB, Du ZY, Engling G, Liu JM, Ma YL, Zheng M, Weber RJ (2016) The characteristics of brown carbon aerosol during winter in Beijing. Atmos Environ 127:355–364
Chow JC, Watson JG, Kuhns HD, Etyemezian V, Lowenthal DH, Crow DJ, Kohl SD, Engelbrecht JP, Green MC (2004) Source profiles for industrial, mobile, and area sources in the Big Bend Regional Aerosol Visibility and Observational (BRAVO) Study. Chemosphere 54:185–208
Collaud Coen M, Weingartner E, Apituley A, Ceburnis D, Fierz-Schmidhauser R, Flentje H, Henzing JS, Jennings SG, Moerman M, Petzold A, Schmid O (2010) Minimizing light absorption measurement artifacts of the aethalometer: evaluation of five correction algorithms. Atmos Meas Tech 3:457–474
Desyaterik Y, Sun YL, Shen XH, Lee TH, Wang XF, Wang T, Collett JL (2013) Speciation of "brown" carbon in cloud water impacted by agricultural biomass burning in eastern China. J Geophys Res 118:7389–7399
Drinovec I, Močnik G, Zotter P, Prévôt A, Ruckstuhl C, Coz E, Rupakheti M, Sciare J, Müller T, Wiedensohler A (2014) The "dual-spot" aethalometer: an improved measurement of aerosol black carbon with real-time loading compensation. Atmos Meas Tech Discuss 7:10179–10220
Favez O, Haddad EI, Piot C, Borêave A, Abidi E, Marchand N, Jaffrezo JL, Besombes JL, Personnaz MB, Sciare J, Wortham H, George C, D'Anna B (2010) Inter-comparison of source apportionment models for the estimation of wood burning aerosols during wintertime in an Alpine city (Grenoble, France). Atmos Chem Phys 10(12):5295–5314
Gao B, Wang XM, Zhao XY, Zhao XY, Ding X, Fu XX, Zhang YL, He QF, Zhang Z, Liu TY, Huang ZZ, Chen LG, Peng Y, Guo H (2015) Source apportionment of atmospheric PAHs and their toxicity using PMF: impact of gas/particle partitioning. Atmos Environ 103:114–120
Guo CF, Wu YS, Chen JC, Fu PPC, Chang CN, Ho TT, Chen MH (2005) Characteristic study of polycyclic aromatic hydrocarbons for fine and coarse particulates at Pastureland near Industrial Park sampling site of central Taiwan. Chemosphere 60:427–433
Hecobian A, Zhang X, Zheng M, Frank N, Edgerton ES, Weber RJ (2010) Water-soluble organic aerosol material and the light-absorption characteristics of aqueous extracts measured over the Southeastern United States. Atmos Chem Phys 10:5965–5977
Hoffer A, Gelencser A, Guyon P, Kiss G, Schmid O, Frank GP, Artaxo P, Andreae MO (2006) Optical properties of humic-like substances (HULIS) in biomass-burning aerosols. Atmos Chem Phys 6:3563–3570
Jacobson MZ (1999) Isolating nitrated and aromatic aerosols and nitrated aromatic gases as sources of ultraviolet light absorption. J Geophys Res 104:3527–3542
Lack DA, Langridge JM (2013) On the attribution of black and brown carbon light absorption using the Ångstrom exponent. Atmos Chem Phys 13:10535–10543
Lack DA, Langridge JM, Bahreini R, Cappa CD, Middlebrook AM, Schwarz JP (2012) Brown carbon and internal mixing in biomass burning particles. Proc Natl Acad Sci U S A 109:14802–14807
Laskin J, Laskin A, Nizkorodov SA, Roach P, Eckert P, Gilles MY, Wang B, Lee HJ, Hu Q (2014) Molecular selectivity of brown carbon chromophores. Environ Sci Technol 48:12047–12055
Laskin A, Laskin J, Nizkorodov SA (2015) Chemistry of atmospheric brown carbon. Chem Rev 115(10):4335–4382
Liu J, Bergin M, Guo H, King L, Kotra N, Edgerton E, Weber RJ (2013) Size-resolved measurements of brown carbon in water and methanol extracts and estimates of their contribution to ambient fine-particle light absorption. Atmos Chem Phys 13:12389–12404
Meng Y, Anderson JL (2010) Tuning the selectivity of polymeric ionic liquid sorbent coatings for the extraction of polycyclic aromatic hydrocarbons using solid-phase microextraction. J Chromatogr A 1217(40):6143–6152
Mesquita SR, van Drooge BL, Reche C, Guimaraes L, Grimalt JO, Barata C, Pina B (2014) Toxic assessment of urban atmospheric particle-bound PAHs: relevance of composition and particle size in Barcelona (Spain). Environ Pollut 184(1):555–562
Olson MR, Victoria Garcia M, Robinson MA, Van Rooy P, Dietenberger MA, Bergin M, Schauer JJ (2015) Investigation of black and brown carbon multiple-wavelength-dependent light absorption from biomass and fossil fuel combustion source emissions. J Geophys Res 120(13):6682–6697
Rajput P, Sarin M, Rengarajan R (2011) High-precision GC-MS analysis of atmospheric polycyclic aromatic hydrocarbons (PAHs) and isomer ratios from biomass burning emissions. J Environ Prot 2(2):445–453
Saleh R, Robinson ES, Tkacik DS, Ahern AT, Liu S, Auken AC (2014) Brownness of organics in aerosols from biomass burning linked to their black carbon content. Nature 7:647–650
Sandradewi J, Prevôt ASH, Szidat S, Perron N, Alfarra MR, Lanz VA, Weingartner E, Baltensperger U (2008) Using aerosol light absorption measurements for the quantitative determination of wood burning and traffic emission contributions to particulate matter. Environ Sci Technol 42:3316–3323
Sawicki E (1962) Analysis for airborne particulate hydrons, their relative proportion affected by different types of pollution. Nat Cancer Inst Monogr 9(6):201–208
Shen ZX, Cao JJ, Arimoto R, Han ZW, Zhang RJ, Han YM, Liu SX, Okuda T, Nakao S, Tanaka S (2009) Ionic composition of TSP and $PM_{2.5}$ during dust storms and air pollution. Atmos Environ 43:2911–2918
Shen GF, Wang W, Yang YF, Ding JN, Xue M, Min YJ, Zhu C, Shen HZ, Li W, Wang R, Wang XL, Tao S, Russell AG (2011) Emissions of PAHs from indoor crop residue burning in a typical rural stove: emission factors, size distributions, and gas-particle partitioning. Environ Sci Technol 45(4):1206–1212
Shen ZX, Cao JJ, Zhang LM, Liu L, Zhang Q, Li J, Han YM, Zhu CS, Zhao ZZ, Liu SX (2014) Day–night differences and seasonal variations of chemical species in PM_{10} over Xi'an, northwest China. Environ Sci Pollut Res 21:3697–3705
Shen ZX, Zhang Q, Cao JJ, Zhang LM, Lei YL, Huang Y, Huang RJ, Gao JJ, Zhao ZZ, Zhu CS, Yin YL, Zheng CL, Xu HM, Liu SX (2017) Optical properties and possible sources of brown carbon in $PM_{2.5}$ over Xi'an, China. Atmos Environ 150:322–330
Srinivas B, Sarin MM (2014) Brown carbon in atmospheric outflow from the Indo-Gangetic Plain: mass absorption efficiency and temporal variability. Atmos Environ 89:835–843
Sun J, Shen ZX, Cao JJ, Zhang LM, Wu TT, Zhang Q, Yin XL, Lei YL, Huang Y, Huang RJ, Liu SX, Han YM, Xu HM, Zheng CL, Liu PP (2017) Particulate matters emitted from maize straw burning for winter heating in rural areas in Guanzhong Plain, China: current emission and future reduction. Atmos Res 184:66–76
Tao J, Zhang L, Zhang R, Wu Y, Zhang Z, Zhang X, Tang Y, Cao J, Zhang Y (2016) Uncertainty assessment of source attribution of $PM_{2.5}$ and its water-soluble organic carbon content using different biomass burning tracers in positive matrix factorization analysis—a case study in Beijing. Sci Total Environ 543:326–335
Teich M, van Pinxteren D, Wang M, Kecorius S, Wang Z, Müller T, Močnik G, Herrmann H (2016) Contributions of nitrated aromatic compounds to the light absorption of water-soluble and particulate brown carbon in different atmospheric environments in Germany and China. Atmos Chem Phys Discuss. doi:10.5194/acp-2016-647

Virkkula A, Mäkelä T, HIllamo R, Yli-tuomi T, Hirsikko A, Hämeri K, Koponen IK (2007) A simple procedure for correcting loading effects of aethalometer data. J Air Waste Manag Assoc 57:1214–1222

Watson JG, Chow JC, Houck JE (2001) $PM_{2.5}$ chemical source profiles for vehicle exhaust, vegetative burning, geological material, and coal burning in northwestern Colorado during 1995. Chemosphere 43(8):1141–1151

Zhang X, Lin YH, Surratt JD, Zotter P, Prevôt ASH, Weber RJ (2011) Light absorbing soluble organic aerosol in Los Angeles and Atlanta: a contrast in secondary organic aerosol. J Geophys Res Lett 38:L21810. doi:10.1029/2011GL049385

Zhang T, Cao JJ, Chow JC, Shen ZX, Ho KF, Ho SSH, Liu SX, Han YM, Watson JG, Wang GH, Huang RJ (2014) Characterization and seasonal variations of levoglucosan in fine particulate matter in Xi'an, China. J Air Waste Manag Assoc 64(11):1317–1327

Zhang Q, Shen ZS, Cao JJ, Zhang RJ, Zhang LM, Huang RJ, Zheng CJ, Wang LQ, Liu SX, Xu HM, Zheng CL (2015) Variations in $PM_{2.5}$, TSP, BC, and trace gases (NO_2, SO_2, and O_3) between haze and non-haze episodes in winter over Xi'an, China. Atmos Environ 112:64–71